SLIDING MODE CONTROL WITH LINEAR QUADRATIC REGULATOR AUGMENTED WITH INTEGRATORS APPLIED TO A 2DOF HELICOPTER

Fernando dos Santos Barbosa*, Fabio Yukio Toriumi†, Bruno Augusto Angélico†

*Department of Robotics, Perception and Learning
KTH Royal Institute of Technology
Stockholm, Sweden

†Departamento de Engenharia de Telecomunicações e Controle
Escola Politécnica da Universidade de São Paulo - USP
São Paulo, SP, Brazil

Emails: fdsb@kth.se, fabioyt@usp.br, angelico@lac.usp.br

Abstract— It is proposed the use of Sliding Mode Control (SMC) with Linear Quadratic Regulator (LQR) when augmented with integrators: the former guarantees robustness against model uncertainty and external disturbance while the latter adds tracking capability with null steady-state error for step inputs. Besides, only the first derivative of the reference is required for trajectory tracking. The η-reachability condition is studied for a manifold based on the tracking error. The methodology of inserting integrators at the input of the linear controller is also described, and the proposed control scheme is applied to a 2DOF Helicopter.

Keywords— Integral Sliding Mode, Linear Quadratic Regulator, Trajectory Tracking, 2DOF Helicopter

1 Introduction

Sliding Mode Controllers (SMCs) are part of a class of controllers known as Variable Structure Systems (VSS), in which the control law is modified according to some rules. It presents robustness to matched uncertainties, i.e., external disturbances and model uncertainties that can be related to the control input in the state-space representation (Hamayun et al., 2016).

However, this robustness is only guaranteed while the switching function is zero and the system is in the sliding phase. During the time taken to reach the manifold, named reaching phase, these properties do not stand, and the system stays sensitive to matched uncertainties. Integral Sliding Mode Controllers (ISMC) appeared to cope with this drawback and force the system to slide throughout the entire time, with no reaching phase (Utkin and Shi, 1996).

In both methods, the control signal is formed by a linear and a nonlinear part. The first is responsible for the system performance while the latter rejects perturbations. Applications are influenced by two factors: the first is due to smoothing the switching function in order to limit high frequency oscillations, the second is the necessity of the second derivative of the reference when in tracking mode.

An ISMC is applied to a Two Degrees of Freedom (2DOF) helicopter in Butt and Aschemann (2015), with state estimation by discrete extended Kalman Filter. Although good tracking is achieved by feedback linearization, it still relies on the second derivative of the reference. This helicopter is also used in Ahmed et al. (2010) for applying a 2-SMC super twisting algorithm, which overcomes the chattering caused by the switching function.

A 3DOF helicopter, an underactuated system, is used in Rios et al. (2010) to compare the implementation of a quasi-continuous controller with sliding mode differentiator and a classical PID with sliding mode observer. To test Fault Detection and Isolation schemes in this same prototype, Capello et al. (2016) uses SMC to stabilize the plant. Lastly, a tracking control is developed in (Liu et al., 2012) joining a nonlinear model predictive control (NMPC) with a nonlinear disturbance observer.

The SMC methodology is applied in Xu and Ozguner (2006) to fully control a quadcopter, in which the system model is divided into a fully-actuated subsystem and an under-actuated one. The complete and detailed model of a large quadrotor is developed in Pounds et al. (2010), along with its linearization, discretization, PID control and indoor and outdoor tests. A switching model predictive attitude control based on the piecewise affine quadcopter mode is presented in Alexis et al. (2011).

It is proposed in this paper a control scheme that combines the ISMC with LQR augmented with integrators, formulated below.

2 Control Formulation

A widely known Sliding Mode Controller is described in Slotine and Li (1991), which uses feedback linearization along with the part dependent on the switching function. It proposes an Integral Sliding Mode manifold in the following form:

$$\sigma(t) = \dot{\tilde{x}}(t) + 2\lambda\tilde{x}(t) + \lambda^2 \int_0^t \tilde{x}(\tau)d\tau, \qquad (1)$$

with λ being a design positive constant that drives the surface to zero and $\tilde{x}(t) = x(t) - x^d(t)$ being the tracking error, i.e., the difference between the actual state and the desired one. This equation can be rearranged to

$$\sigma(t) = \begin{bmatrix} 2\lambda & 1 & \lambda^2 \end{bmatrix} \begin{bmatrix} \tilde{x}(t) \\ \dot{\tilde{x}}(t) \\ \int_0^t \tilde{x}(\tau)d\tau \end{bmatrix}, \qquad (2)$$

which has two interesting characteristics:

- it is in the form $\sigma(t) = \mathbf{G}\mathbf{x}(t)$, another SMC design methodology based on the linear states of the system (Hamayun et al., 2016);
- the state vector is equivalent to the one used on Linear Quadratic Regulators (LQR) with integrators inserted at the input.

2.1 LQR with Integrators

Consider the following state-space system

$$\dot{\mathbf{x}}(t) = \mathbf{A}\mathbf{x}(t) + \mathbf{B}\mathbf{u}(t) \qquad (3)$$
$$\mathbf{y}(t) = \mathbf{C}\mathbf{x}(t), \qquad (4)$$

with $\mathbf{x}(t)$ being the state vector, $\mathbf{y}(t)$ the output vector, $\mathbf{u}(t)$ the control signal and $\mathbf{A}$, $\mathbf{B}$ and $\mathbf{C}$ the state, input and output matrices, respectively. The Linear Quadratic Regulator is an optimal controller, such that $\mathbf{u}(t) = -\mathbf{K}\mathbf{x}(t)$, with $\mathbf{K}$ being the feedback gain matrix that minimizes the following index

$$J = \int_0^\infty \left(\mathbf{x}^T(t)\mathbf{Q}\mathbf{x}(t) + \mathbf{u}^T(t)\mathbf{R}\mathbf{u}(t)\right) dt, \qquad (5)$$

in which $\mathbf{Q}$ is a real symmetric positive semi-definite matrix and $\mathbf{R}$ is a real symmetric positive definite matrix, and they weigh the relative importance of the states' errors and the energy consumption by the controller. This is known as Regulator Form, as presented in Fig. 1, since the objective is stabilizing the states at the linearization point.

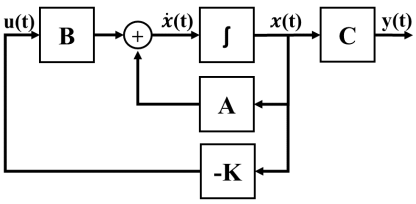

Figure 1: Block diagram of the LQR in regulation form.

As a matter of fact, it is possible to prove that the optimal control law that satisfies the quadratic performance index is given by (Ogata, 2001; Skogestad and Postlethwaite, 2007)

$$\mathbf{u}(t) = -\mathbf{K}\mathbf{x}(t) = -\mathbf{R}^{-1}\mathbf{B}^T\mathbf{P}\mathbf{x}(t), \qquad (6)$$

with $\mathbf{P}$ being the solution of the following Riccati equation

$$\mathbf{A}^T\mathbf{P} + \mathbf{P}\mathbf{A} - \mathbf{P}\mathbf{B}\mathbf{R}^{-1}\mathbf{B}^T\mathbf{P} + \mathbf{Q} = \mathbf{0}. \qquad (7)$$

Integrators can be inserted to allow the system to track a reference, as presented in Fig. 2.

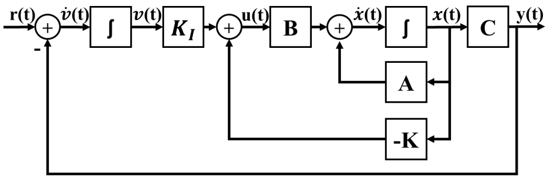

Figure 2: Block diagram of the LQR with integrator insertion.

The control signal is now defined as

$$\mathbf{u}(t) = -\mathbf{K}\mathbf{x}(t) + \mathbf{K}_I\mathbf{v}(t), \qquad (8)$$

with $\mathbf{K}_I$ being the integrator gain matrix and $\mathbf{v}(t)$ the output integrator vector, and the integrator equation is given by

$$\dot{\mathbf{v}}(t) = \mathbf{r}(t) - \mathbf{y}(t) = \mathbf{r}(t) - \mathbf{C}\mathbf{x}(t). \qquad (9)$$

The closed-loop equation can be written as

$$\begin{bmatrix} \dot{\mathbf{x}}(t) \\ \dot{\mathbf{v}}(t) \end{bmatrix} = \begin{bmatrix} \mathbf{A} - \mathbf{B}\mathbf{K} & \mathbf{B}\mathbf{K}_I \\ -\mathbf{C} & \mathbf{0} \end{bmatrix} \begin{bmatrix} \mathbf{x}(t) \\ \mathbf{v}(t) \end{bmatrix} + \begin{bmatrix} \mathbf{0} \\ \mathbf{I} \end{bmatrix} \mathbf{r}(t), \qquad (10)$$

from which it is possible to show that

$$\begin{bmatrix} \mathbf{A} - \mathbf{B}\mathbf{K} & \mathbf{B}\mathbf{K}_I \\ -\mathbf{C} & \mathbf{0} \end{bmatrix} = \underbrace{\begin{bmatrix} \mathbf{A} & \mathbf{0} \\ -\mathbf{C} & \mathbf{0} \end{bmatrix}}_{\mathbf{A}_{aug}} - \underbrace{\begin{bmatrix} \mathbf{B} \\ \mathbf{0} \end{bmatrix}}_{\mathbf{B}_{aug}} \underbrace{\begin{bmatrix} \mathbf{K} & -\mathbf{K}_I \end{bmatrix}}_{\mathbf{K}_{aug}}. \qquad (11)$$

Thus, an LQR controller can be designed for the augmented state-space system, defined by matrices $\mathbf{A}_{aug}$, $\mathbf{B}_{aug}$, $\mathbf{C}_{aug} = \begin{bmatrix} \mathbf{C} & \mathbf{0} \end{bmatrix}$ and $\mathbf{x}_{aug}(t) = \begin{bmatrix} \mathbf{x}(t) & \mathbf{v}(t) \end{bmatrix}^T$. Moreover, the augmented control law is given by

$$\mathbf{u}_{aug}(t) = -\mathbf{K}_{aug}\mathbf{x}_{aug}(t). \qquad (12)$$

2.2 Integral Sliding Mode

Let a Linear Time-Invariant (LTI) system, already augmented with integrators as presented in the previous section, be written as

$$\dot{\mathbf{x}}_{aug}(t) = \mathbf{A}_{aug}\mathbf{x}_{aug}(t) + \mathbf{B}_{aug}\mathbf{u}(t) + \mathbf{B}_{aug}\mathbf{D}\xi(t,x) \qquad (13)$$

with $\mathbf{x}_{aug}(t)$ being the state vector, $\mathbf{u}(t)$ the control signal, $\mathbf{A}_{aug}$ and $\mathbf{B}_{aug}$ the state and input matrices, respectively, and $\mathbf{D}\xi(t,x)$ represents the model uncertainty or external disturbance. A typical sliding mode control law is

$$\mathbf{u}(t) = \mathbf{u}_l(t) + \mathbf{u}_n(t), \qquad (14)$$

in which $\mathbf{u}_l(t)$ comes from the LQR with integrator on the input and $\mathbf{u}_n(t)$ from a nonlinear one; the former is chosen to be an LQR feedback gain, while the latter corresponds to a switching function. Then,

$$\mathbf{u}(t) = -\mathbf{K}_{aug}\mathbf{x}_{aug}(t) - \rho(t,x)(\mathbf{G}\mathbf{B}_{aug})^{-1}\frac{\sigma(t)}{\|\sigma(t)\|}, \tag{15}$$

and $\sigma(t)$ is the sliding surface, $\mathbf{G}$ is a matrix to be designed such that $(\mathbf{G}\mathbf{B}_{aug})^{-1}$ is invertible and $\rho(t,x)$ such that guarantees the sliding condition.

Let us propose a surface $\sigma(t)$ dependent on the tracking error, i.e., on the difference between the actual states $\mathbf{x}_{aug}(t)$ and the desired ones, $\mathbf{x}^d_{aug}(t)$:

$$\sigma(t) = \mathbf{G}\left(\mathbf{x}_{aug}(t) - \mathbf{x}^d_{aug}(t)\right). \tag{16}$$

Differentiating this equation yields

$$\begin{aligned}\dot{\sigma}(t) &= \mathbf{G}\left[\dot{\mathbf{x}}_{aug}(t) - \dot{\mathbf{x}}^d_{aug}(t)\right] \qquad (17)\\ &= \mathbf{G}\left[\mathbf{A}_{aug}\mathbf{x}_{aug}(t) + \mathbf{B}_{aug}\mathbf{u}_l(t) + \mathbf{B}_{aug}\mathbf{u}_n(t) + \right.\\ &\qquad \left. \mathbf{B}_{aug}\mathbf{D}\xi(t,x) - \dot{\mathbf{x}}^d_{aug}(t)\right], \qquad (18)\end{aligned}$$

and replacing (15) on its results, after some simplification, in

$$\dot{\sigma}(t) = \mathbf{G}\left[\left(\mathbf{A}_{aug} - \mathbf{B}_{aug}\mathbf{K}_{aug}\right)\mathbf{x}_{aug}(t) - \dot{\mathbf{x}}^d_{aug}(t)\right] - \rho(t,x)\frac{\sigma(t)}{\|\sigma(t)\|} + \mathbf{G}\mathbf{B}_{aug}\mathbf{D}\xi(t,x). \tag{19}$$

The linear controller should guarantee that the first part of this equation tends to zero, allowing us to simplify it to

$$\dot{\sigma}(t) = -\rho(t,x)\frac{\sigma(t)}{\|\sigma(t)\|} + \mathbf{G}\mathbf{B}_{aug}\mathbf{D}\xi(t,x). \tag{20}$$

Multiplying (20) on the left by $\sigma^T(t)$ and using the fact that $\sigma^T(t)\sigma(t) = \|\sigma(t)\|^2$ gives us

$$\begin{aligned}\sigma^T(t)\dot{\sigma}(t) &= -\rho(t,x)\|\sigma(t)\| + \sigma^T(t)\mathbf{G}\mathbf{B}_{aug}\mathbf{D}\xi(t,x)\\ &\le \|\sigma(t)\|\left(-\rho(t,x) + \|\mathbf{G}\mathbf{B}_{aug}\mathbf{D}\xi(t,x)\|\right).\end{aligned} \tag{21}$$

So, choosing $\rho(t,x)$ as

$$\rho(t,x) \ge \|\mathbf{G}\mathbf{B}_{aug}\mathbf{D}\xi(t,x)\| + \eta \tag{22}$$

satisfies the multivariable version of the Sliding Condition (η-reachability) (Hamayun et al., 2016)

$$\sigma^T(t)\dot{\sigma}(t) \le -\eta\|\sigma(t)\|. \tag{23}$$

For a single-input single-output (SISO) system, (16) can be written as

$$\sigma(t) = \begin{bmatrix} G_1 & G_2 & G_3 \end{bmatrix}\begin{bmatrix} \tilde{x}(t) \\ \dot{\tilde{x}}(t) \\ \int_0^t \tilde{x}(\tau)d\tau \end{bmatrix}, \tag{24}$$

which, when changing to state variables, becomes

$$\sigma(t) = G_1x_1(t) + G_2x_2(t) + G_3x_3(t), \tag{25}$$

and knowing that $\dot{x}_3(t) = x_1(t)$ and $\ddot{x}_3(t) = \dot{x}_1(t) = x_2(t)$ gives us the following

$$\sigma(t) = G_2\ddot{x}_3(t) + G_1\dot{x}_3(t) + G_3x_3(t), \tag{26}$$

from which is possible to state that the sliding manifold corresponds to a second order system. Thus, matrix $\mathbf{G}$ defines the manifold dynamics.

For multivariable systems, one way of choosing $\mathbf{G}$ would be such that it generates uncoupled manifolds, even for coupled systems. As an example, let us define a system with two outputs, $a(t)$ and $b(t)$. Their sliding manifolds can be written as

$$\sigma(t) = \begin{bmatrix} G_1^a & 0 & G_2^a & 0 & G_3^a & 0 \\ 0 & G_1^b & 0 & G_2^b & 0 & G_3^b \end{bmatrix}\begin{bmatrix} \tilde{a}(t) \\ \tilde{b}(t) \\ \dot{\tilde{a}}(t) \\ \dot{\tilde{b}}(t) \\ \int_0^t \tilde{a}(\tau)d\tau \\ \int_0^t \tilde{b}(\tau)d\tau \end{bmatrix}. \tag{27}$$

Another method is presented in Castanos and Fridman (2006), which proposes choosing $\mathbf{G}$ in order to avoid amplifying unmatched disturbances and is given by

$$\mathbf{G} = \left(B^T_{aug}B_{aug}\right)^{-1}B^T_{aug}. \tag{28}$$

3 2DOF Helicopter Application

A 2DOF Helicopter was used to apply the proposed control technique. It is a good application example as it has two inputs and two outputs with coupled dynamics. Its nonlinear equation of motion may be written as (Quanser, 2011; Neto et al., 2016):

$$\ddot{\theta} = \frac{K_{pp}A_pPWM_p + K_{py}A_yPWM_y - \alpha - B_p\dot{\theta}}{J_{eq\_p} + m_{heli}l^2_{cm}}, \tag{29}$$

$$\alpha = m_{heli}l_{cm}\cos(\theta)\left[l_{cm}\sin(\theta)\dot{\psi}^2 + g\right]; \tag{30}$$

$$\ddot{\psi} = \frac{K_{yp}A_pPWM_p + K_{yy}A_yPWM_y + \beta - B_y\dot{\psi}}{J_{eq\_y} + m_{heli}\cos(\theta)^2l^2_{cm}}, \tag{31}$$

$$\beta = 2m_{heli}l^2_{cm}\sin(\theta)\cos(\theta)\dot{\psi}\dot{\theta}; \tag{32}$$

in which θ and ψ are pitch and yaw angles, respectively, m_{heli} is the helicopter weight and l_{cm} the distance from center of mass to center of rotation. PWM is the motor signal percentage, B the air resistance factor and J_{eq} the inertia, with subscripts p and y standing for pitch and yaw, respectively, which are also used on K_{ab}, standing for the torque on 'a' produced by motor 'b' squared velocity. PWM is related to the motors squared speeds, Ω_p^2 and Ω_y^2, by linear approximation, with slopes being A_p and A_y.

By writing the state vector as $\mathbf{x}(t) = \begin{bmatrix}\theta & \psi & \dot{\theta} & \dot{\psi}\end{bmatrix}^T$ and the input vector as $\mathbf{u}(t) = \begin{bmatrix}PWM_p & PWM_y\end{bmatrix}^T$, the linearized version of equations (29) to (32), around the operation point $\begin{bmatrix}0 & 0 & 0 & 0\end{bmatrix}^T$, can be written as

$$\dot{\mathbf{x}}(t) = \mathbf{A}\mathbf{x}(t) + \mathbf{B}\mathbf{u}(t) + \mathbf{B}\mathbf{D}\xi(t,x), \tag{33}$$

with

$$\mathbf{A} = \begin{bmatrix} 0 & 0 & 1 & 0 \\ 0 & 0 & 0 & 1 \\ 0 & 0 & \dfrac{-B_p}{J_{eq\_p} + m_{heli}l_{cm}^2} & 0 \\ 0 & 0 & 0 & \dfrac{-B_y}{J_{eq\_y} + m_{heli}l_{cm}^2} \end{bmatrix}, \tag{34}$$

$$\mathbf{B} = \begin{bmatrix} 0 & 0 \\ 0 & 0 \\ \dfrac{K_{pp}A_p}{J_{eq\_p} + m_{heli}l_{cm}^2} & \dfrac{K_{py}A_y}{J_{eq\_p} + m_{heli}l_{cm}^2} \\ \dfrac{K_{yp}A_p}{J_{eq\_y} + m_{heli}l_{cm}^2} & \dfrac{K_{yy}A_y}{J_{eq\_y} + m_{heli}l_{cm}^2} \end{bmatrix}, \tag{35}$$

$$\mathbf{D}\xi(t,x) = \begin{bmatrix} \dfrac{-K_{yy}\alpha + K_{py}\beta}{A_p(K_{pp}K_{yy} - K_{py}K_{yp})} \\ \dfrac{K_{yp}\alpha + K_{pp}\beta}{A_y(K_{pp}K_{yy} - K_{py}K_{yp})} \end{bmatrix}. \tag{36}$$

Fig. 3 displays the custom built 2DOF Helicopter[1]; it uses two Brushless DC motors (BLDC) with fixed-pitch propellers as actuators, 2 rotary encoders as sensors and a NXP FRDM-K64F development board for embedded processing.

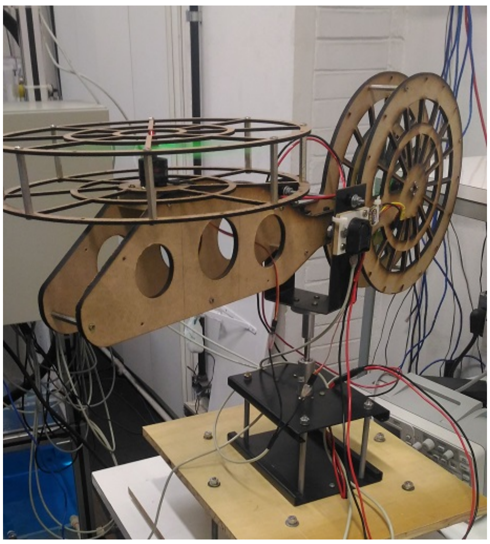

Figure 3: Custom built 2DOF Helicopter.

[1] A video of this plant can be watched on Youtube: `www.youtube.com/watch?v=E84x9rKRSSo`.

The system parameters are presented in Table 1.

Table 1: Helicopter Parameters

Parameter	**Value**	**Unit**
m_{heli}	1.317	kg
l_{cm}	0.038	m
K_{pp}	0.0180	N.m/%
K_{yy}	-0.0033	N.m/%
K_{py}	-6.35×10^{-4}	N.m/%
K_{yp}	10.76×10^{-4}	N.m/%
B_p	0.1	N/%
B_y	0.1	N/%
J_{eq_p}	0.384	kg.m^2
J_{eq_y}	0.0432	kg.m^2

In order to reduce chattering and high-order frequency switching of the nonlinear part of the controller, the following sigmoidal approximation is used

$$\mathbf{u}(t) = -\mathbf{K}\mathbf{x}(t) - \rho(t,x)(\mathbf{G}\mathbf{B})^{-1}\frac{\sigma(t)}{\|\sigma(t)\| + \delta}, \tag{37}$$

being δ a small positive scalar.

The following test procedure is used:

- at 15s, a step reference of 0.35rad is given to pitch;
- a -1rad reference in given to yaw at 30s;
- references for pitch and yaw are changed to zero at 45s and 60s, respectively.

Fig. 4a presents the system response to the test procedure and Fig. 4b shows the control effort. Figures 4c and 4d depict pitch and yaw sliding manifolds, respectively, and then Figures 5a and 5b show zoomed parts of each manifold.

The major manifolds peaks in Figures 4c and 4d are caused by the step references, but it is clear that they quickly returns to zero. The minor peaks from Figures 5a and 5b are mainly due to sensor imprecision and derivative approximation used to calculate axes speeds.

4 Conclusion

This work described the use of Linear Quadratic Regulators (LQR) with integrators inserted at the input of the controller along with a Sliding Mode Controller. The proposed controller presents two benefits: it is capable of guaranteeing null steady-state error for step inputs and the second derivative of the reference signal is not required. A 2DOF Helicopter was used to obtain experimental results. It was observed that the controller was able to perfectly track the reference signal. Future work will deal with Output Sliding Mode Control.

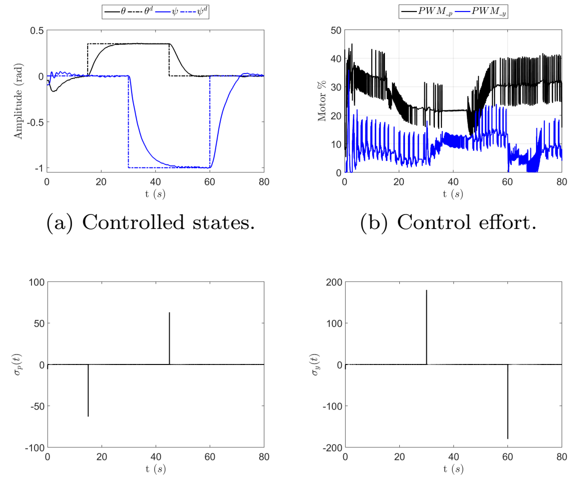

(a) Controlled states. (b) Control effort.

(c) Pitch angle sliding manifold. (d) Yaw angle sliding manifold.

Figure 4: Practical results from the controller applied to the built helicopter.

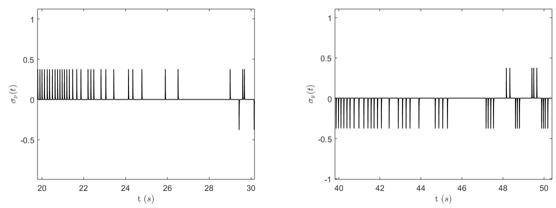

(a) Fig. 4c with zoom. (b) Fig. 4d with zoom.

Figure 5: Zoomed parts of pitch and yaw sliding manifolds.

Acknowledgment

Authors acknowledge the contribution of Fundação de Amparo à Pesquisa do Estado de São Paulo (FAPESP) under the grant 2017/22130-4.

References

Ahmed, Q., Bhatti, A. I., Iqbal, S. and Kazmi, I. H. (2010). 2-sliding mode based robust control for 2-dof helicopter, *2010 11th International Workshop on Variable Structure Systems (VSS)*, pp. 481–486.

Alexis, K., Nikolakopoulos, G. and Tzes, A. (2011). Switching model predictive attitude control for a quadrotor helicopter subject to atmospheric disturbances, *Control Engineering Practice* **19**(10): 1195 – 1207.

Butt, S. S. and Aschemann, H. (2015). Multivariable integral sliding mode control of a two degrees of freedom helicopter, *IFAC-PapersOnLine* **48**(1): 802 – 807.

Capello, E., Punta, E. and Fridman, L. (2016). Strategies for control, fault detection and isolation via sliding mode techniques for a 3-dof helicopter, *2016 IEEE 55th Conference on Decision and Control (CDC)*, pp. 6464–6469.

Castanos, F. and Fridman, L. (2006). Analysis and design of integral sliding manifolds for systems with unmatched perturbations, *IEEE Transactions on Automatic Control* **51**(5): 853–858.

Hamayun, M. T., Edwards, C. and Alwi, H. (2016). *Fault Tolerant Control Schemes Using Integral Sliding Modes*, Springer International Publishing.

Liu, C., Chen, W.-H. and Andrews, J. (2012). Tracking control of small-scale helicopters using explicit nonlinear mpc augmented with disturbance observers, *Control Engineering Practice* **20**(3): 258 – 268.

Neto, G. G., Barbosa, F. d. S. and Angélico, B. A. (2016). 2-dof helicopter controlling by pole-placements, *2016 12th IEEE International Conference on Industry Applications (INDUSCON)*, pp. 1–5.

Ogata, K. (2001). *Modern Control Engineering*, 4th edn, Prentice Hall PTR.

Pounds, P., Mahony, R. and Corke, P. (2010). Modelling and control of a large quadrotor robot, *Control Engineering Practice* **18**(7): 691 – 699. Special Issue on Aerial Robotics.

Quanser (2011). *Quanser 2-DOF Helicopter - Laboratory Manual*, 2.0 edn, Quanser Inc.

Rios, H., Rosales, A., Ferreira, A. and Davilay, A. (2010). Robust regulation for a 3-dof helicopter via sliding-modes control and observation techniques, *Proceedings of the 2010 American Control Conference*, pp. 4427–4432.

Skogestad, S. and Postlethwaite, I. (2007). *Multivariable feedback control: analysis and design*, Vol. 2, Wiley New York.

Slotine, J.-J. E. and Li, W. (1991). *Applied Nonlinear Control*, Pearson.

Utkin, V. and Shi, J. (1996). Integral sliding mode in systems operating under uncertainty conditions, *Proceedings of 35th IEEE Conference on Decision and Control*, Vol. 4, pp. 4591–4596.

Xu, R. and Ozguner, U. (2006). Sliding mode control of a quadrotor helicopter, *Proceedings of the 45th IEEE Conference on Decision and Control*, pp. 4957–4962.